# Single-molecule confocal microscopy studies of electric-field induced orientation in chromophore-polymer composite materials

D. R. B. Sluss, P. M. Wallace, K. D. Truong, B. H. Robinson, L. R. Dalton,
and P. J. Reid*
Box 351700, Department of Chemistry, University of Washington, Seattle, WA 98195

## ABSTRACT

Chromophore-polymer composite materials for electro-optical applications are rendered active at the $\chi^{(2)}$ level of susceptibility by inducing chromophore alignment through the interaction of the chromophore dipole moment with an external electric field, a process referred to as "poling". To provide insight into the molecular details of the poling process, single molecule microscopy studies of DCM (4-(dicyanomethylene)-2-methyl-6-(4-dimethylaminostyryl)-4*H*-pyran) and RhB (Rhodamine B) in poly(methyl acrylate) (PMA) above $T_g$ of the polymer host are performed. Electric fields of 50 V/μm are employed consistent with typical experimental conditions. The effect of environment is studied through comparative studies or RhB reorientation in oxidative and inert atmospheres. Single-molecule rotational dynamics are monitored through the time-evolution of the fluorescence anisotropy. Anisotropy correlation functions demonstrate non-exponential decay consistent with previous studies of molecular rotation dynamics in polymer melts. The rotational dynamics of DCM are found to be weakly perturbed in the presence of a 50 V/μm electric field consistent with the modest alignment potential created by the electric field relative to the amount of available thermal energy. The relevance of these findings to current models of the poling process is discussed.

**Keywords:** single-molecule microscopy, rotational dynamics, electric-field effects, non-linear optical materials

## 1. INTRODUCTION

Recent advances in organic photonic materials suggest that these materials will play an important role in next generation electro-optical (EO) devices.[1-15] These materials hold the potential of higher switching frequencies and lower operational voltages when compared to current inorganic materials (i.e., $LiNO_3$). However, fulfilling the promise of these materials requires a molecular-level understanding of the issues that limit their efficiency. A central issue surrounding the development of organic EO materials is the translation of molecular systems of large hyperpolarizabilties, $\beta$, into macroscopic assemblies possessing large EO activity.[7,13] The EO response is one of several effects derived from the $\chi^{(2)}$ level of susceptibility.[16] Chromophore-polymer composite materials lack inherent non-centrosymmetry which is required for finite $\chi^{(2)}$ response. In chromophore-polymer composite systems, material non-centrosymmetry is established through the use of an external electric field or "poling" field which induces chromophore alignment through interaction with the molecular dipole moment ($\mu$). In the typical poling process, the polymer composite is heated near the glass transition temperature ($T_g$) allowing the chromophores to reorient in response to the poling field. The composite is then cooled below $T_g$ in order to preserve the field-induced chromophore alignment. The extent of EO activity is related to $\beta$ and the extent of molecular order as follows:[14]

$$\mathrm{EO} \propto N\beta\left\langle \cos^3\theta \right\rangle \tag{1}$$

where $N$ is the chromophore number density and $\left\langle \cos^3\theta \right\rangle$ is the chromophore orientation parameter. Equation (1) suggests that one strategy for optimizing EO activity is to maximize the extent of molecular order. This requires a detailed understanding of the poling process.

*Author to whom correspondence should be addressed. preid@chem.washington.edu

Linear and Nonlinear Optics of Organic Materials VI, edited by Robert A. Norwood,
Proc. of SPIE Vol. 6331, 63310K, (2006) · 0277-786X/06/$15 · doi: 10.1117/12.674778

Theoretical techniques have been used to explore the details of the poling process, and these studies have shown that in the dilute chromophore limit, the extent of molecular order is dependent on the product of the molecular dipole moment and poling field strength ($E$) versus the amount of thermal energy available, or simply $\mu E/kT$.[16-24] The field strengths investigated were generally much greater than $kT$ in contrast to experimental conditions where dielectric breakdown limits usable poling fields to ≤100 V/μm corresponding to regimes in which $\mu E < kT$. In addition, the computational studies generally employ a gas phase lattice model in which the environment provided by the polymer host is assumed to be homogeneous, and the interactions between the chromophore and host matrix are ignored. The influence of spatial heterogeneity that typifies polymer environments remains an open issue with respect to poling efficacy. Experimental techniques capable of following molecular reorientation dynamics in polymer environments especially under experimentally-relevant poling conditions are required to evaluate these models, and to provide further insight into the molecular details operative in the poling process.

Polarization-sensitive confocal microscopy allows one to measure the spatial orientation and rotational dynamics of single molecules.[25-36] This technique has been used to measure the rotational dynamics of rhodamine dyes in polymers at temperatures slightly above $T_g$.[27,29,31,33,34] These experiments were designed to determine the contribution of spatial and temporal homogeneity to the complex rotational dynamics observed in polymers close to $T_g$. Non-exponential rotational correlation decay dynamics were observed consistent with environmental heterogeneity of the polymer environment. In addition, two polymers were studied at similar temperatures relative to $T_g$ and the molecular rotational dynamics were found to differ between the two polymer hosts.[29] This observation indicates that the poling temperature relative to $T_g$ may not be the only parameter that influences molecular reorientation in response to the poling field.

We present here a series of single-molecule confocal microscopy studies of chromophore rotational dynamics in chromophore-polymer composite materials. The effects of molecular shape, electric field poling, and environment are investigated through single molecule microscopy of DCM (4-(dicyanomethylene)-2-methyl-6-(4-dimethylaminostyryl)-4*H*-pyran) and RhB (Rhodamine B) in poly(methyl acrylate) (PMA) above $T_g$. Electric fields of 50 V/μm are employed consistent with typical experimental poling conditions. The effect of environment is studied through comparative studies or RhB reorientation in oxidative and inert atmospheres. The observed single-molecule rotational dynamics for DCM and RhB are analyzed to determine the change in rotational dynamics with external perturbation. We find that the chromophore rotational dynamics are non-exponential, consistent with previous studies of molecular rotation dynamics in polymers suggesting that the dynamical heterogeneity of the polymer environment influences chromophore reorientation. The addition of gaseous $N_2$ to the RhB composites results in a modest alteration of the rotational dynamics presumably due to a change in the blinking dynamics. In the presence of the poling field, the rotational dynamics of DCM are modestly perturbed consistent with the fact that the amount of available thermal energy is greater than the potential energy of interaction between the molecular dipole and applied field. The relevance of these results with respect to current models of the poling process is discussed.

## 2. EXPERIMENTAL

**2.1 Sample Preparation.** The laser dyes DCM (4-(dicyanomethylene)-2-methyl-6-(4-dimethylaminostyryl)-4*H*-pyran, Aldrich 98%) and Rhodamine B (RhB, Sigma 95%) were used as received. Stock solutions of the dyes at a concentration of 4 x $10^{-9}$ M and 20 wt% poly-methyl acrylate (PMA, Aldrich, MW ~40 kD, $T_g$ = 303 K) were both prepared in cyclopentanone (Aldrich ≥ 99%). Structures of the compounds used in this study are presented in Figure 1. The polymer solution was mixed for 24 hours then filtered (Whatman, 0.45 μm) before use. The dye and polymer solutions were mixed in a 1:4 ratio resulting in a final concentration of 1 x $10^{-9}$ M in 15 wt% polymer solution. This concentration provided for a molecular number density consistent with single-molecule resolution. The samples were deposited on glass coverslips (Corning No.1 25 x 25 mm) by spin coating. Before use the coverslips were cleaned in a boiling solution of 3:2:1 deionized (DI) water :ammonium hydroxide :hydrogen peroxide for one hour and then rinsing with DI water and dried with gaseous nitrogen. In the electric-field studies, aluminum electrodes designed for poling in a *x,y* geometry suitable for single-molecule microscopy were fabricated on glass coverslips. Details of the electrode fabrication procedure are provided elsewhere.[37] Electrodes were fabricated with a

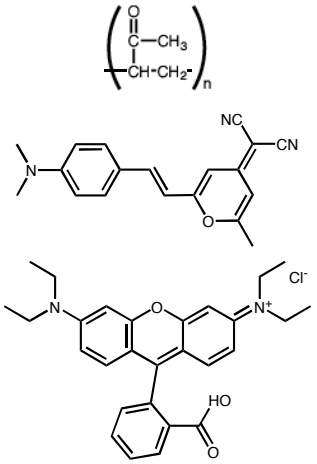


**Figure 1.** Chemical structures for PMA (top), DCM (middle) and RhB (bottom).

roughly 10 μm gap to withstand a 50 V/μm electric field generated with a high voltage power supply[37] A 100-μL aliquot of the sample solution was deposited onto the electrode assembly by spin coating at 3000 rpm for 30 seconds, and the resulting film thickness (200 nm) was measured by surface profilemetry (Dektak 3030). The samples were held overnight under vacuum before use.

**2.2 Single Molecule Confocal Microscopy.** Single molecule microscopy studies were preformed using an inverted scanning fluorescence confocal microscope described in detail elsewhere.[37] Photoexcitation was accomplished using the 532-nm output from a Nd:$YVO_4$ laser (Spectra Physics Millennia V). The laser output was converted to circular polarization using a λ/4 waveplate. Excitation powers of ≤10 μW were employed for DCM, and ≤800 nW for RhB with the difference in power reflecting the difference in absorption cross section at 532 nm . Images were acquired by scanning the sample with 100-nm resolution in both the *x* and *y* directions over the focal volume of the microscope. The polarization components of the fluorescence were obtained and detected using a polarizing beamsplitter and two avalanche photodiode detectors (PerkinElmer, SPCM-AQR-16). The depolarized fluorescence from dye-doped polystyrene spheres (Molecular Probes) was measured daily allowing for normalization of the detector outputs. For experiments performed under an inert atmosphere, upon removal from the vacuum oven the samples were flushed with gaseous nitrogen which remained flowing over the sample during the measurements. All of the data were collected at an ambient room temperatures which were 20 ± 1 ºC for DCM corresponding to $T_g$ + 11 ºC, and 23 ± 1 ºC for RhB corresponding to $T_g$ + 14 ºC.

## 3. RESULTS

**3.1 Single-Molecule Emission.** In this study the influence of an applied electric field on molecular orientation is studied by monitoring the fluorescence dichrosim of single molecules. However, it is well known that the high-NA objectives employed in single-molecule studies mix the polarization components of the fluorescence.[38-40] Therefore, the effect of the objective on the measured dichroism must be considered. In this study the excitation field is circularly polarized such that all transition-dipole orientations in the xy-plane of the microscope are excited. The objective collects the molecular fluorescence, and relays this emission through a polarizing beam splitter that separates it into its dichroic components. The effect of high-NA objectives on the measured dichroic components of the emission has been discussed in the literature, and the following expressions for the experimentally observed dichroic components of the emission, $I_{\parallel}$ and $I_{\perp}$, have been derived:[37]

$$\begin{aligned} I_{\parallel} &= K_1\mu_x^2 + K_2\mu_y^2 + K_3\mu_z^2 \\ I_{\perp} &= K_2\mu_x^2 + K_1\mu_y^2 + K_3\mu_z^2 \end{aligned} \tag{2}$$

In Equation (2), $K_1$, $K_2$, and $K_3$ define the extent of emission polarization mixing defined by the NA of the objective employed. In this work, a 1.3 NA oil-immersion objective ($n$ = 1.518) dictates that $\theta_{obj}$ = 59º. With this angle, $K_1$, $K_2$, and $K_3$ are equal to:

$$\begin{aligned} K_1 &= \frac{1}{4}\left(5 - 3\cos\theta_{obj} - \cos^2\theta_{obj} - \cos^3\theta_{obj}\right) = 2.393 \\ K_2 &= \frac{1}{12}\left(1 - 3\cos\theta_{obj} + 3\cos^2\theta_{obj} - \cos^3\theta_{obj}\right) = 0.0296 \\ K_3 &= \frac{1}{3}\left(2 - 3\cos\theta_{obj} + \cos^3\theta_{obj}\right) = 0.616 \end{aligned} \tag{3}$$

To recast Equation (2) in matrix form, we make the following definitions:

$$\vec{I} = \begin{pmatrix} I_{\parallel} \\ I_{\perp} \end{pmatrix}; \quad \vec{\varepsilon} = \begin{pmatrix} 1 \\ 1 \end{pmatrix}; \quad \underset{\sim}{K} = \begin{pmatrix} K_1 & K_2 \\ K_2 & K_1 \end{pmatrix}$$

With these definitions Equation (2) becomes:

$$\bar{I} = \underset{\sim}{K}\begin{pmatrix}\mu_x^2\\ \mu_y^2\end{pmatrix} + K_3\bar{\varepsilon}\mu_z^2 \tag{4}$$

In the above expression, the molecular transition dipole moment is expressed in the frame of the optical system. The optical-system frame is related to the molecular frame by a standard Euler rotation:

$$\bar{\mu} = R(\Omega)\begin{pmatrix}0\\ 0\\ |\mu_o|\end{pmatrix} = |\mu_o|\begin{pmatrix}\sin\theta\cos\varphi\\ \sin\theta\sin\varphi\\ \cos\theta\end{pmatrix} \tag{5}$$

The definition of $\bar{\mu}$ provided by Equation (5) is then related to the fluorescence intensity in terms of the rotation angles defining the orientation of the transition dipole in the molecular frame:

$$\bar{I} = |\mu_o|^2\left\{\sin^2\theta\,\underset{\sim}{K}\begin{pmatrix}\cos\varphi^2\\ \sin\varphi^2\end{pmatrix} + K_3\bar{\varepsilon}\cos^2\theta\right\} \tag{6}$$

The matrix equation can be simplified by using the $\underset{\sim}{K}$ matrix to transform the intensities in an effort to partially undo the polarization mixing introduced by the objective:

$$\bar{\Im} = \underset{\sim}{K}^{-1}\bar{I} = |\mu_o|^2\left\{\sin^2\theta\begin{pmatrix}\cos\varphi^2\\ \sin\varphi^2\end{pmatrix} + \kappa\bar{\varepsilon}\cos^2\theta\right\} \tag{7}$$

where $\underset{\sim}{K}^{-1}$ and $\kappa$ are equal to:

$$\underset{\sim}{K}^{-1} = \frac{1}{K_1^2 - K_2^2}\begin{pmatrix}K_1 & -K_2\\ -K_2 & K_1\end{pmatrix};\quad \kappa = \frac{K_3}{K_1 + K_2} \tag{8}$$

The new intensities, $\bar{\Im}$, may be considered to be partially back transformed from the object frame to the molecular frame. The correction factor, $\kappa = 0.229$ for the present case, represents the extent to which this approach does not fully remove the effects of the large NA objective. However, taking the difference between the back-transformed parallel and perpendicular intensities (as done in constructing the linear anisotropy below) has the effect of removing this correction. The sum of the two polarization components of the emission will contain the correction, but will not demonstrate any dependence on the minor Euler angle. Expressing this result with respect to the equilibrium probability distribution of the angles, $P_{eq}(\theta,\varphi)$, yields

$$\begin{aligned}|\mu_o|^{-2}\left\langle\left(\Im_{\parallel} - \Im_{\perp}\right)\right\rangle &= \left\langle\sin^2\theta\cos 2\varphi\right\rangle\\ |\mu_o|^{-2}\left\langle\left(\Im_{\parallel} + \Im_{\perp}\right)\right\rangle &= \left\langle\sin^2\theta + 2\kappa\cos^2\theta\right\rangle\end{aligned} \tag{9}$$

In the poling process, the presence of an electric field is expected to bias the molecular orientation distribution towards the direction of the electric field. The magnitude of this interaction is dependent on both the magnitude of the molecular dipole moment and the applied field. The molecule of interest in this study, DCM, possesses a dipole moment of ~10 D and fields of 50 V/μm are employed. The field is parallel to the *X* axis of the optical system; therefore, the equilibrium

probability distribution is no longer uniform over all orientations. The orientational distribution will be governed by the Boltzmann probability distribution:

$$P_{eq}(\theta,\varphi) = \frac{e^{f\cos\varphi}}{\iint_{\theta,\varphi} e^{f\cos\varphi}\sin\theta d\theta d\varphi} \tag{10}$$

In Equation (10), $f$ is equal to $\mu E/kT$ where $\mu$ is the magnitude molecular dipole moment, $E$ is the magnitude of the poling field, $k$ is Boltzmann's constant, and $T$ is temperature. For the experimental conditions of this study:

$$f = \frac{\mu E}{kT} \approx 0.4 \tag{11}$$

Using this result, the effect of the poling field on the bulk averaged dichorsim is given by:

$$\begin{aligned}
&|\mu_o|^{-2}\left\langle\left(\Im_{\parallel}-\Im_{\perp}\right)\right\rangle = \left\langle\sin^2\theta\left(\cos^2\varphi-\sin^2\varphi\right)\right\rangle = \tfrac{1}{2}\left\langle\cos 2\varphi\right\rangle \\
&|\mu_o|^{-2}\left\langle\left(\Im_{\parallel}+\Im_{\perp}\right)\right\rangle = \left\langle\sin^2\theta+2\kappa\cos^2\theta\right\rangle = \tfrac{1}{2}\left(1+2\kappa\right) \\
&\left\langle\left(\cos^2\varphi-\sin^2\varphi\right)\right\rangle \approx \tfrac{1}{8}f^2 \\
&\left\langle\cos 2\varphi\right\rangle = \frac{\int_{\varphi=0}^{2\pi}\cos 2\varphi\cdot e^{f\cos\varphi}d\varphi}{\int_{\varphi=0}^{2\pi} e^{f\cos\varphi}d\varphi}
\end{aligned} \tag{12}$$

**3.2 Reduced Linear Dichroism.** As demonstrated in previous studies of chromophores in polymer melts, the rotational dynamics of the chromophore can be described through the time evolution of the emission dichroism expressed as the reduced dichroism, $A(t)$: [27]

$$A_I(t) = \frac{I_{\parallel}(t)-I_{\perp}(t)}{I_{\parallel}(t)+I_{\perp}(t)} \tag{13}$$

The anisotropy ratio in terms of the back-transformed intensities is defined as as:

$$A_{\Im}(t) = \frac{\Im_{\parallel}(t)-\Im_{\perp}(t)}{\Im_{\parallel}(t)+\Im_{\perp}(t)} \tag{14}$$

Using the above definitions we find:

$$A_{\Im}(t) = \frac{\Im_{\parallel}(t)-\Im_{\perp}(t)}{\Im_{\parallel}(t)+\Im_{\perp}(t)} = \cos 2\varphi\frac{\sin^2\theta}{\sin^2\theta+2\kappa\cos^2\theta} = \cos 2\varphi\frac{1}{1+2\kappa\cot^2\theta} \tag{15}$$

As the orientation of the molecule changes in time, the anisotropy ratio will evolve in time. This form of the anisotropy is nearly the same as the $\cos 2\varphi$, with the correction factor scaled by the parameter, $\kappa$, which is a function of the objective NA. The rotational dynamics as reflected by $A(t)$ can be quantified by the autocorrelation of this quantity, defined as $C(t)$, which is calculated as follows:

$$C(t) = \frac{\sum_{t=0}^{T} A(0)\,A(0+t)}{\left|A(0)\right|^2} \tag{16}$$

where $A(t)$ can be determined using $A_I(t)$ or $A_{\Im}(t)$. The temporal behavior of $C(t)$ demonstrates non-exponential decay; therefore, the temporal evolution of this function generally fit using the Kholrausch-William-Watts (KWW) stretched-exponential function [27,45]:

$$C(t) = \exp\left[-\left(t/\tau_{\mathrm{KWW}}\right)^{\beta}\right] \tag{17}$$

In Equation (17), $\tau_{\mathrm{KWW}}$ is the apparent decay constant and $\beta$ can range from 0 to 1 with $\beta = 1$ representing single exponential decay expected for Brownian rotational diffusion. We will refer to $\beta$ as $\beta_{\mathrm{KWW}}$ throughout the text to avoid confusion with the molecular hyperpolarizability. The weighted average time scale, $\tau_c$, produces a measure of the single-molecule rotation times and is related to $C(t)$ as follows.

$$\tau_c = \int_0^{\infty} C(t)\,dt = \frac{\tau_{\mathrm{KWW}}}{\beta_{\mathrm{KWW}}}\Gamma\left(\frac{1}{\beta_{\mathrm{KWW}}}\right) \tag{18}$$

Finally, the ensemble-averaged correlation time, $\langle\tau_c\rangle$, is calculated from the distribution of weighted average times as follows:

$$\langle\tau_c\rangle = \frac{1}{N}\sum_{i=1}^{N}(\tau_c)_i \tag{19}$$

**3.3 Single-Molecule Microscopy Results.** A 5 x 5 μm image of the fluorescence from single RhB molecules in PMA is presented in Figure 2. The 300-nm diameter of the molecular images reflects the near-diffraction limited focus of the laser. Single molecules were located by performing a raster scan of the sample until the measured intensity from both channels exceeded a preset threshold value. When this threshold was exceeded, scanning was paused and the intensity on both detectors was monitored as a function of time for up to 200 seconds. Figures 3 and 4 illustrate the analysis required to connect the fluorescence intensity data to the molecular rotation dynamics for such a threshold event for DCM and RhB, respectively. In Figures 3A and 4A, $I_{\parallel}(t)$ and $I_{\perp}(t)$ measured for a representative threshold event are shown. Fluctuations in intensities between the polarization components are observed due to molecular rotation until permanent loss of signal occurs due to photodestruction. Figures 3B and 4B are an expanded view of the first 25 s of the data shown in panels 3A and 4A, and anticorrelation of the observed intensities is evident consistent with molecular rotation. Using $I_{\parallel}$ and $I_{\perp}$, $A(t)$ is calculated as described by Equation (13), and presented in Figures 3C and 4C. The autocorrelation of $A(t)$ before the photodestruction event, $C(t)$ is shown in Figures 3D and 4D. Consistent with previous studies of molecular rotational dynamics in polymer melts, the decay of $C(t)$ for DCM and RhB are not well described by single-exponential decay as illustrated by the mismatch

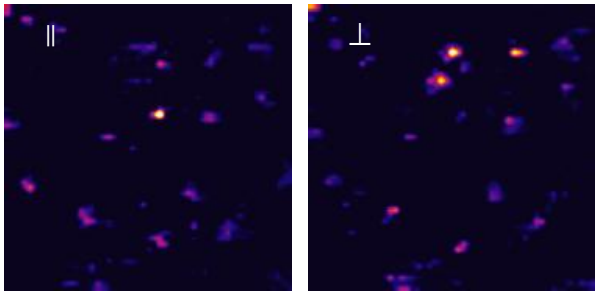


**Figure 2.** False-color images of the flourescence of single RhB molecules. The figure represents a $5 \times 5$ μm$^2$ scan employing 0.1 μm steps of 10-9 M RhB in 15 wt% PMA. The fluorescence is polarized parallel to the applied electric field (above left) or perpendicular (above right). The color scale corresponds to counts of 20-200 per 100 ms time window.

between the exponential fit (dashed lines) and data (black diamonds) . In contrast, the data are better fit by the stretched exponential function (solid lines) with $\tau_{KWW}$ = 0.15 s and $\beta_{KWW}$ = 0.79 for the DCM molecule and $\tau_{KWW}$ = 0.28 s and $\beta_{KWW}$ = 0.84 for the RhB molecule.

For DCM in the absence of the poling field, $\tau_{KWW}$ was found to vary between 0.05 – 0.89 s with $\langle \tau_{KWW} \rangle = 0.25 \pm 0.02$ s, and values of $\beta_{KWW}$ ranged between 0.5 and 1 with $\langle \beta_{KWW} \rangle = 0.83 \pm 0.01$. Histograms of $\tau_{KWW}$ and $\beta_{KWW}$ in the presence and absence of the poling field are presented in Figures 5A and 5B. The deviation of $\beta_{KWW}$ from 1 suggests the rotational dynamics are reflecting the heterogeneous environment provided by the polymer host; however, the preponderance of values lie between 0.7 and 1 demonstrating that the rotational dynamics are near exponential. The effect of an external electric field on the rotational dynamics of DCM ($\tau_c$) was determined by comparing the weighted average correlation times as calculated using Equation (18) for molecules in the presence and absence of the poling field. Figure 5C presents the values of $\tau_c$ determined for 99 molecules in the absence of an applied external field, and for 120 molecules in the presence of a 50 V/μm field. Although the histograms with and without the external field are similar, a shift to higher $\tau_c$ values is observed in the presence of the poling field. This slight enhancement in $\tau_c$ is reflected by the

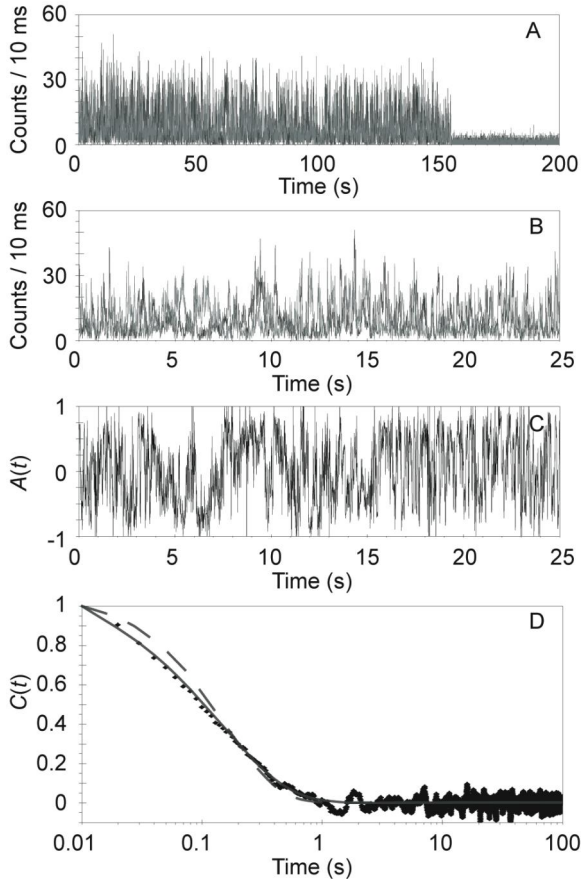


**Figure 3.** A typical single molecule time trace of DCM in PMA ($T_g$ = 11 °C). Panel A presents the signal for the two dichroic components of the fluorescence (|| to the electric field as light gray, ⊥ as dark grey). A single-step bleach at 150 s is observed, consistent with single-molecule photodestruction. In panel B, the first 25 s of the evolution in panel A is shown to more clearly depict the rotational dynamics. The reduced linear dichrosim, $A(t)$, is illustrated in panel C. Panel D is a fit to the autocorrelation of the transient showing both an exponential fit (dashed, $\tau$ = 0.16 s) and a fit to Equation (17) (solid, $\tau_{KWW}$ = 0.15 s and $\beta_{KWW}$ = 0.78).

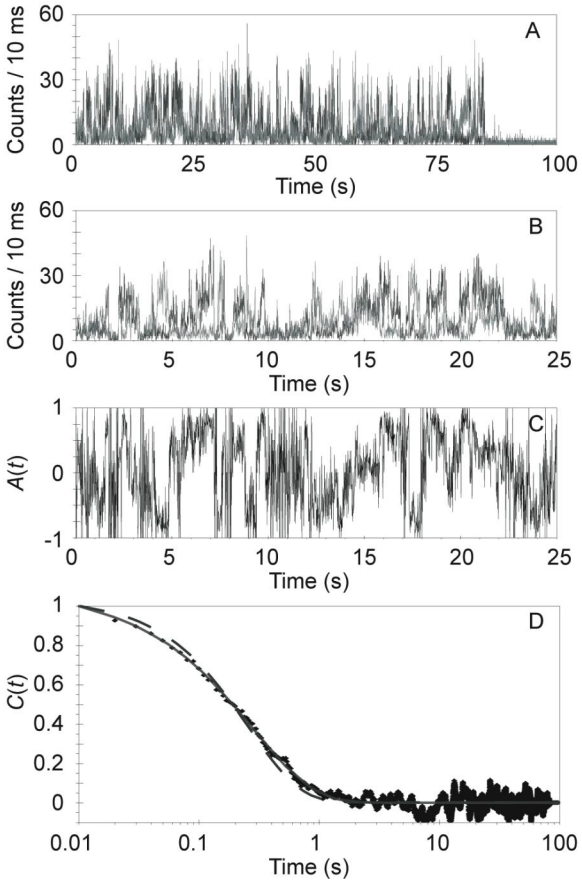


**Figure 4.** A typical single molecule time trace of RhB in PMA ($T_g$ = 14 °C). Panel A presents the signal for the two dichroic components of the fluorescence (|| to the electric field as light gray, ⊥ as dark grey). A single-step bleach at 85 s is observed, consistent with single-molecule photodestruction. In panel B, the first 25 s of the evolution in panel A is shown to more clearly depict the rotational dynamics. The reduced linear dichrosim, $A(t)$, is illustrated in panel C. Panel D is a fit to the autocorrelation of the transient showing both an exponential fit (dashed, $\tau$ = 0.26 s) and a fit to Equation (17) (solid, $\tau_{KWW}$ = 0.28 s and $\beta_{KWW}$ = 0.84).

average correlation times $\left(\left\langle \tau_c \right\rangle\right)$ of 0.29 ± 0.02 s and 0.33 ± 0.03 s in the absence and presence of the electric field, respectively.

An alternate way to gauge the effect of an applied field is illustrated in Figure 5D. Here, histograms of the ratio of $I_{\parallel}$ to $I_{\perp}$ averaged over the molecule's lifetime are shown in the presence and absence of the electric field. The application of the poling field is expected to bias the molecular alignment in the direction of the field; therefore, this should be reflected by an increase in the dichroic ratio in the presence of the electric field. The average intensity ratio is 0.98 ± 0.02 with no external field, and in the presence of a 50 V/μm field the average ratio undergoes a sight increase to 1.00 ± 0.03. In addition, the histogram in the presence of the electric field demonstrates broadening and skewing of the intensity ratio to values greater than unity and is consistent with a biasing of the molecular orientation in the direction of the electric field.

For RhB molecules in an ambient atmosphere, values of $\tau_{KWW}$ ranged from 0.13 to 2.28 s with $\left\langle \tau_{KWW} \right\rangle = 0.45 \pm 0.03$ s, and values of $\beta_{KWW}$ ranged from 0.57 to 1 with $\left\langle \beta_{KWW} \right\rangle = 0.82 \pm 0.01$. Histograms of $\tau_{KWW}$ and $\beta_{KWW}$ for RhB in ambient atmosphere and in the presence of nitrogen gas are presented in Figures 5E and F. When compared to DCM under nearly identical conditions, $\beta_{KWW}$ is strikingly similar with the molecules exhibiting the same near-exponential rotational dynamics. However, the $\tau_{KWW}$ histograms differ in that the values for RhB extend to much longer correlation times. This behavior is reflected in $\left\langle \tau_{KWW} \right\rangle$ for RhB that is almost double that of DCM. The effect of an inert environment on the rotational dynamics was studied using RhB single molecules. 135 and 143 molecules were interrogated under normal atmospheric conditions in the lab and under nitrogen gas respectively.

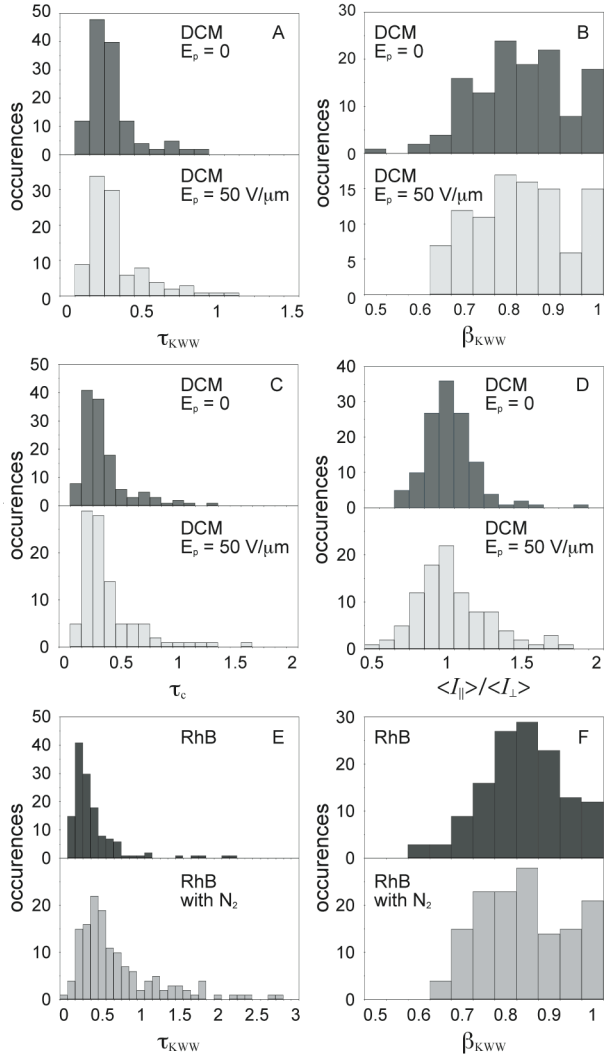


**Figure 5.** Histograms for the fit parameters ($\tau_{KWW}$ in panel A and $\beta_{KWW}$ in panel B, single-molecule correlation time ($\tau_c$ panel C), and $<I_{\parallel}>/<I_{\perp}>$ (panel D) for DCM are shown along with the fit parameters ($\tau_{KWW}$ in panel E and $\beta$ in panel F) for RhB. The values with no perturbation are shown on top of each panel, and on the bottom are values in the presence of a 50 ± 5 V/$\mu$m electric field for DCM and gaseous $N_2$ for RhB.

## 4. DISCUSSION

**4.1 Comparative Rotational Dynamics.** The distributions of $\tau_{KWW}$ presented in Figures 5A and 5E are consistent with the heterogeneous environment of the polymer host causing variations in molecular rotational dynamics between individual probe molecules. Comparison of the rotational dynamics for DCM and RhB demonstrates that the structure of the probe molecule has some influence on the measured dynamics. Specifically, the shapes of the $\tau_{KWW}$ histograms are similar (Figures 5A and 5E); however, $\left\langle \tau_{KWW} \right\rangle$ for DCM in PMA is roughly half (250 ms) the corresponding value for RhB (450 ms). Rotational correlation times have been shown to vary for different probe molecules in the same polymer.[46] Therefore, differences in probe molecule geometry or alteration of the intermolecular interactions with the polymer host may be responsible for the differences in $\left\langle \tau_{KWW} \right\rangle$. With respect to molecular interactions, the $\beta_{KWW}$ distributions are nearly identical for DCM and RhB suggesting that the dynamical heterogeneity of the polymer host is reflected to a similar extent in the rotational dynamics of both probe molecules. The distribution of $\beta_{KWW}$ provides

information on the distribution of rotational environments experienced by the probe molecules. Since the structure and electrostatic properties of DCM and RhB are quite different with DCM being dipolar and having a prolate geometry while RhB is charged and has an oblate geometry, the interactions with the surrounding polymer should differ and potentially result in different $\beta_{KWW}$ distributions. However, the similarity in $\beta_{KWW}$ demonstrates that differences in interaction have limited effect on the rotational dynamics, and instead the difference in $\langle\tau_{KWW}\rangle$ reflects variation in the molecular rotational dynamics accompanying the different structures of the probe molecules.

Comparing RhB samples that were interrogated under ambient and nitrogen conditions, near-exponential decays of $C(t)$ are observed in both environments. As shown in Figure 5F, both RhB $\beta_{KWW}$ histograms show a very similar distribution possessing the same mean of 0.82. As much as $\beta_{KWW}$ does not change when the sample is introduced to a nitrogen environment, $\tau_{KWW}$ did show some surprising differences. Specifically, the distribution for $\tau_{KWW}$ in $N_2$ is shifted to longer times and possesses more outliers. With the addition of the nitrogen environment, these differences in the histograms are reflected in values of $\langle\tau_{KWW}\rangle$ which increases from 0.45 s to 0.76 s in the presence of $N_2$. The motivation for exploring the effect of a nitrogen environment on the molecular rotational dynamics is the increased time before photodesctruction and a potential decrease in blinking dynamics. The increase in $\langle\tau_{KWW}\rangle$ is consistent with modification of these quantities. However, molecules included for analysis were required to survive for at least 20 times $\langle\tau_{KWW}\rangle$; therefore, the decreased rate of photodestruction in $N_2$ is presumably not responsible for the increase in $\langle\tau_{KWW}\rangle$. Instead, the increased time suggests that blinking dynamics have some impact on the value of $\langle\tau_{KWW}\rangle$.

The largest difference observed here relative to other studies of single-molecule rotation dynamics in polymer melds is the near-exponential decay of $C(t)$ and $\beta_{KWW}$ that range from 0.7 to 1.0. We argued previously that the near-exponential decay of DCM[37] as opposed to the non-exponential decay reported for rhodamine derivatives[27-29,31] was due to differences in molecular geometry. However, our results on RhB do not support this argument. Instead, probe-specific rotational dynamics may be responsible for the differences in $C(t)$ and $\beta_{KWW}$ between studies. Wang and Richert have recently demonstrated that for probe molecules in glass forming liquids, if the rotational time constant of the probe is significantly greater than the structural relaxation time of the surrounding environment, the rotational dynamics of the probe as reflected by decay of the linear anisotropy will demonstrate exponential decay.[47] In this case, the observation of exponential decay is due to the rotational correlation function reflecting the average environment experienced by the probe. Although only a few measurements of the dielectric relaxation in PMA exist, the relaxation near the glass transition temperature as described within the Kohlrausch-Williams-Watts law is consistent with an average relaxation time of 0.15 s.[48] Since the temperature employed in this study is above $T_g$, the relaxation time for the polymer will presumably be on a shorter timescale. Given this, the near-exponential decay of the rotational correlation observed here may reflect the rapid fluctuations of the polymer host relative to the slower rotational dynamics of the probe.

Tomczak et al. have performed similar measurements of the rhodamine derivative tetramethylrhodamine-5-isothio-cyanate (5-TRITC) in PMA.[31] In this study, the polarization components of multiple single molecules were simultaneously measured using wide-field microscopy. An average value of approximately 0.6 was found for $\beta_{KWW}$ with the distribution of values ranging from 0.1 to 1. Compared to the values of $\beta_{KWW}$ reported here, the Tomczak rotational decay curves demonstrate significantly greater non-exponential behavior in contrast to the near-exponential decay observed here. Although 5-TRITC is similar in structure to RhB, 5-TRITC has an extra N=C=S functional group that may alter the electrostatic properties of the molecule. Second, sample size may also be an issue. The investigations of Tomczak et al. involved 35 molecules compared to the 135 RhB molecules studied here. Therefore, the differences between the studies may be due to limited sampling of the molecular ensemble.

**4.2 Poling Effects on Chromophore Orientation.** The results presented here demonstrate that at the temperature employed in this study, DCM molecules in PMA experienced significant rotational mobility. This behavior is consistent with the expected enhanced rotational mobility when $T > T_g$.[33,49-52] As shown in Figures 5C and 5D, the relative similarity of $\langle\tau_c\rangle$ and $\langle I_{\parallel}\rangle/\langle I_{\perp}\rangle$ in the presence and absence of the poling field demonstrated that the molecular rotational dynamics of DCM are only slightly perturbed by the presence of the electric field. This observation could be

viewed as surprising within the context of current conceptual descriptions of the poling process. These descriptions are largely derived from theoretical studies that have predicted significant field-induced molecular order for poling fields in excess of 100 V/μm.[13,16,18-24] However, the poling field used in this study, 50 V/μm, is representative of typical fields employed in device construction. Given a poling field of this magnitude and the dipole moment of DCM (10 D), $\mu E$ is approximately equal to $0.4kT$. Therefore, the amount of thermal energy available to DCM is significantly greater than the electrostatic potential energy created by the poling field. This energetic comparison is consistent with the observation that the poling field provides only a modest perturbation to the rotational dynamics of DCM.

The extent of the electric-field perturbation on molecular orientation can be placed in more quantitative terms. The intensity-ratio distributions presented in Figure 5D demonstrate a slight alteration in the presence of the poling field. For an isotropic medium in the absence of an electric field, the time averaged value, $\langle I_{\parallel} \rangle / \langle I_{\perp} \rangle$ or more precisely $\langle \Im_{\parallel} \rangle / \langle \Im_{\perp} \rangle$, should be unity. With the application of a poling field, molecular orientation in the direction of the field will be favored, and the ratio should become greater than unity. Using Equations (7) and (12) the effect of the poling field on molecular orientation as reflected by the fluorescence polarization intensity ratio expressed in terms of $f$ is:

$$\frac{\langle\langle \Im_{\parallel} \rangle\rangle}{\langle\langle \Im_{\perp} \rangle\rangle} = \frac{1 + 2\kappa + \frac{1}{8} f^2}{1 + 2\kappa - \frac{1}{8} f^2} \tag{20}$$

In the experiments performed here, DCM experienced a poling field of 50 V/μm such that $f \sim 0.4$, and from Equation (20) a slight, 2% increase in the intensity ratio is expected in presence of the poling field. An increase of this magnitude is consistent with the ratio data presented in Figure 5D. This simple analysis demonstrates that many more single molecules would need to be interrogated to definitively measure an intensity ratio shift of this size. This behavior is largely due to the fact that linear dichroism is an even function of the molecular orientation parameter (i.e., $\cos^2 \varphi$) such that linear dependence on $f$ vanishes in Equation (20) by symmetry leaving $f^2$ as the lowest-order field dependence reflected by this measurement. In contrast, $\chi^{(2)}$ techniques, such as second-harmonic generation, are dependent and are odd functions of molecular orientation (i.e., $\cos^3 \varphi$), such that linear $f$ dependence is reflected by these techniques, thereby providing a more sensitive measure of orientation for modest values of the poling field and molecular dipole moment.

## ACKNOWLEDGEMENTS

The National Science Foundation is acknowledged for their support of this work through the Science and Technology Center for Materials and Devices for Information Technology Research (DMR 0120967). Support from DARPA is also acknowledged. PJR is an Alfred P. Sloan Fellows and is a Cottrell Scholar of the Research Corporation.

## REFRENCES

(1) D.M. Burland, R.D. Miller, C.A. Walsh, "Second-Order nonlinearity in poled-polymer systems," *Chem. Rev.*, **94**, 31-78, 1994.

(2) S.R. Marder, W.E. Torruellas, M. Blanchard-Desce, V. Ricci, G.I. Stegeman, S. Gilmour, J. Brédas J. Li, G.U. Bublitz, S.G. Boxer, "large molecular third-order optical nonlinearities in polarized carotenoids," *Science*, **276**, 1233-1236, 1997.

(3) D. Chen, H.R. Fetterman, A. Chen, W.H. Steier, L.R. Dalton, W. Wang, Y. Shi, "Demonstration of 110 GHz electro-optic polymer modulators," *Appl. Phys. Lett.*, **70**, 3335-3337, 1997.

(4) A. Chen, V. Chuyanov, H. Zhang, S. Garner, S. Lee, W.H. Steier, J. Chen, F. Wang, J. Zhu, M. He, Y. Ra, S.S.H. Mao, A.W. Harper, L.R. Dalton, H.R. Fetterman, "DC biased electro-optic polymer waveguide modulators with low half-wave voltage and high thermal stability," *Opt. Eng.*, **38**, 2000-20008, 1999.

(5) L. Dalton, A. Harper, A. Ren, F. Wang, G. Todorova, J. Chen, C. Zhang, M. Lee, "Polymeric Electro-optic Modulators: From Chromophore Design to Integration with Semiconductor Very large scale integration electronics and silica fiber optics," *Ind. Eng. Chem Res.*, **38**, 8-33, 1999.

(6) A.W. Harper, S. Sun, L.R. Dalton, S.M. Garner, A. Chen, S. Kalluri, W.H. Steier, B.H. Robinson, "Translating microscopic nonlinearity into macroscopic optical nonlinearity: the role of chromophore-chromophore interactions," *J. Opt. Soc. Am. B*, **15**, 329-337, 1998.
(7) B.H. Robinson, L.R. Dalton, A.W. Harper, A. Ren, F. Wang, C. Zhang, G. Todorova, M. Lee, R. Aniszfeld, S. Garner, A. Chen, W.H. Steier, S. Houbrecht, A. Persoons, I. Ledoux, J. Zyss, A.K.Y Jen, "The molecular and supramolecular engineering of polymeric electro-optic materials," *Chem. Phys.*, **245**, 35-50, 1999.
(8) L. Dalton, *Advances in Polymer Science*, 1-86, Springer-Verlag, Berlin, 2002.
(9) K.A. Firestone, P. Reid, R. Lawson, S. Jang, L.R. Dalton, "Advances in organic elecrto-optic materials and processing," *Inorg. Chim. Acta.*, **357**, 3957-3966.
(10) C.W. Spangler, M. He, E.G. Nickel, J. Laquindanum, L.R. Dalton, N. Tang, R. Hellwarth, "The design of new organic materials with enhanced nonlinear optical properties," *Mol. Cryst. Liq. Cryst.*, **240**, 17-23, 1994.
(11) C.W. Spangler, M. He, P. Liu, E.G. Nickel, J. Laquindanum, L.R. Dalton, "The design of new organic materials with enhanced nonlinear optical properties: incorporation of bipolaronic charge states," *Nonlinear Optics*, **10**, 147-152, 1995.
(12) W. Wang, D. Chen, H.R. Fetterman, Y. Shi, W.H. Steier, L.R. Dalton, P.D. Chow, "Optical heterodyne detection of 60 GHz electro-optic modulation from polymer waveguide modulators," *Appl. Phys. Lett*H, **67**, 1806-1808, 1995.
(13) Y. Shi, C. Zhang, H. Zhang, J.H. Bechtel, L.R. Dalton, B.H. Robinson, W.H. Steier, "Low (sub-1-volt) halfwave voltage polymeric elecrto-optic modulators achieved by controlling chromophore shape," *Science*, **288**, 119-122, 2000.
(14) P.N. Prasad, D.J. Williams, *Introduction to Nonlinear Optical Effects in Molecules and Polymers*, John Wiley & Sons, New York, 1991.
(15) A. Galvan-Gonzalez, G.I. Stegeman, A.K.Y. Jen, X. Wu, M. Canva, A.C. Kowalczyk, X.Q. Zhang, H.S. Lackritz, S. Marder, S. Thayumanavan, G. Levina, "Photostability of electro-optic polymers possessing chromophores with efficient amino donors and cyano-containing acceptors," *J. Opt. Soc. Am. B*, **18**, 1846-1853, 2001.
(16) B.H. Robinson, L.R. Dalton, "Monte Carlo statistical mechanical simulations of the competition of intermolecular electrostatic and poling field interactions in defining macroscopic electro-optic activity for organic chromophore/polymer materials," *J. Phys. Chem. A*, **104**, 4785-4795, 2000.
(17) Y.R. Shen, *The Principles of Nonlinear Optics*, John Wiley & Sons: New York, 1984.
(18) Y.V. Pereverzev, O.V. Prezhdo, L.R. Dalton, "A model of phase transitions in the system of electro-optical dipolar chromophores subject to an electric field," *Phys. Rev. B*, **117**, 3354-3369, 2002.
(19) Y.V. Pereverzev, O.V. Prezhdo, L.R. Dalton, "Macroscopic order and electro-optic response of dopolar chromophore-polymer materials," *ChemPhysChem*, **5**, 1821-1830, 2004.
(20) K.D. Singer, M.G. Kuzyk, J.E. Sohn, "Second order nonlinear-optical processes in orientationally ordered materials: relationship between molecular and macroscopic properties," *J. Opt. Soc. Am. B*, **4**, 698-976, 1987.
(21) C.P.J.M. Vandervorst, S.J. Picken, "Electric field poling of acceptor-donor molecules," *J. Opt. Soc. Am. B*, **7**, 320-325, 1990.
(22) F. Ghebremichael, M.G. Kuzyk, K.D. Singer, J.H. Andrews, "Relationship between the second-order microscopic and macroscopic nonlinear optical susceptibilities of poled dye-doped polymers," *J. Opt. Soc. Am. B*, **15**, 2294-2297, 1998.
(23) W. Kim, L.M. Hayden, "Fully atomistic modeling of an electric field poled guest-host nonlinear optical polymer," *J. Chem. Phys.*, **111**, 5212-5222, 1999.
(24) M. Makowska-Janusik, H. Reis, M.G. Papadopoulos, I.G. Economou, N. Zacharopoulos, "Molecular dynamics Simulations of Electric Field Poled Nonlinear Optical Chromophores Incorporated in a Polymer Matrix," *J. Phys. Chem. B*, **108**, 588-596, 2004.
(25) T. Ha, J. Glass, Th. Enderle, D.S. Chemla, S. Weiss, "Hindered rotational diffusion and rotational jumps of single molecules," *Phys. Rev. Lett.*, **80**, 2093-2096, 1998.
(26) T. Ha, T.A. Laurence, D.S Chemla, S. Weiss, "Polarization spectroscopy of single fluorescent molecules," *J. Phys. Chem. B*, **103**, 6839-6850, 1999.
(27) L.A. Deschenes, D.A. Vanden Bout, "Molecular motions in polymer films near the glass transition: a single molecule study of rotational dynamics," *J. Phys. Chem. B*, **105**, 11978-11985 2001.
(28) L.A. Deschenes, D.A. Vanden Bout, "Single-molecule studies of heterogeneous dynamics in polymer melts near the glass transition," *Science*, **292**, 255-258, 2001.

(29) L.A. Deschenes, D.A. Vanden Bout, "Comparison of ensemble and single molecule approaches to probing polymer relaxation dynamics near $T_g$," *J. Chem. Phys.*, **116**, 5850-5856, 2002.
(30) C.R. Viteri, J.W. Gilliland, W.T. Yip, "Probing the dynamics guest-host interactions in sol-gel films using single molecule spectroscopy," *J. Am. Chem. Soc.*, **125**, 1980-1987, 2003.
(31) N. Tomczak, R.A.L. Vallée, E.M.P.H. van Dijk, M. García-Parajó, M.; L. Kuipers, N.F. van Hulst, G.J. Vancso, "Probing polymers with single fluorescent molecules," *Eur. Polym. J.*, **40**, 1001-1011, 2004.
(32) J.T Fourkas, "Rapid determination of the three-dimensional orientation of single molecules," *Opt. Lett.*, **26**, 211-213, 2001.
(33) A.P. Bartko, R.M. Dickson, "Imaging three-dimensional single molecule orientations," *J. Phys. Chem. B*, **103**, 11237-11241, 1999.
(34) A.P. Bartko, K.Xu, R.M. Dickson, " Three-dimensional single molecule rotational diffusion in glassy state polymer films," *Phys. Rev. Lett.*, **89**, 026101, 2002.
(35) J. Hohlbein, C. Hübner, "Simple scheme for rapid three-dimensional orientation determination of the emission dipole of single molecules," *Appl. Phys. Lett.*, **86**, 121104, 2005.
(36) I. Chung, K.T. Shimizu, M.G. Bawendi, "Room temperature measurements of the 3D orientation of single CdSe quantum dots using polarization microscopy," *Proc. Natl. Acad. Sci. U.S.A.*, **100**, 405-408, 2003.
(37) P.M. Wallace, D.R.B. Sluss, L.R. Dalton, B.H. Robinson, P.J. Reid, "Single-molecule microscopy studies of electric-field poling in chromophore-polymer composite materials," *J. Phys. Chem. B*, **110**, 75-82, 2006.
(38) J.T. Fourkas, "Rapid determination of the three-dimensional orientation of single molecules," *Opt. Lett.*, **26**, 211-312, 2001.
(39) G. Hinze, G. Diezemann, Th. Basché, "Rotational correlation functions of single molecules," *Phys. Rev. Lett.*, **93**, 203001, 2004.
(40) C.J. Wei, Y.H. Kim, R.K. Darst, P.J. Rossky, D.A. Vanden Bout, "Origins of Nonexponential decay of single molecule measurements of rotational dyanmics," *Phys. Rev. Lett.*, **95**, 173001, 2005.
(41) C.R. Moylan, S. Ermer, S.M. Lovejoy, I. McComb, D.S. Leung, R. Wortmann, P. Krdmer, R.J. Twieg, "(Dicanomethylene)pyran derivatives with $C_{2v}$ symmetry: an unusual class of nonlinear optical chromophores," *J. Am. Chem. Soc.*, 12950-12955, 1996.
(42) S.L. Bondarev, V.N. Knyukshto, V.I. Stepuro, A.P. Stupak, A.A. Turban, "Fluorescence and electronic structure of the laser dye DCM in solution and in polymethylmethacrlate," *Journal Of Applied Spectroscopy*, **71**, 194-201, 2004.
(43) C. Juang, L. Finzi, C.J. Bustamante, "Design and application of a computer-controlled confocal scanning differential polarization microscope," *Rev. Sci. Instrum.*, **59**, 2399-2408, 1988.
(44) D. Axelrod, "Carbocyanine dye orientation in red cell membrane studied by microscopic florescence polarization," *Biophys. J.*, **26**, 557-573, 1979.
(45) M.D. Ediger, "Spatially heterogeneous dynamics in supercooled liquids," *Annu. Rev. Phys. Chem.*, **52**, 99-128, 2000.
(46) T. Inoue, M.T. Cicerone, N.D. Ediger, "Molecular motions and viscoelasticity of amorphous polymers near $T_g$," *Macromolecules*, **28**, 3425-3433, 1995.
(47) L. Wang, R. Richert, "Exponential probe rotation in glass-forming liquids," *J. Chem. Phys.*, **120**, 11082-11089, 2004.
(48) A. Sanchis, M.G. Prolongo, R.M. Masegosa, R.G. Rubio, "Dynamic-mechanical study of the dynamics of polymer blends near the glass transition," *Macromolecules*, **28**, 2693-2699, 1995.
(49) R.D. Dureiko, D.E. Schuele, K.D. Singer, "Modeling relaxation processes in poled electro-opticc polymer films," *J. Opt. Soc. Am. B*, **15**, 338-348, 1998.
(50) W. Yip, D. Hu, J. Yu, D.A. Vanden Bout, P.F. Barbara, "Classifying the photophysical dynamics of single- and multiple-chromophore molecules by single molecule spectroscopy," *J. Phys. Chem. A*, **102**, 7564-7575, 1998.
(51) M. Stähelin, C.M. Walsh, D.M. Burland, R.D. Miller, R.J. Twieg, W. Volksen, "Orientational decay in poled second-order nonlinear optical guest-host polymers: temperature dependence and effects of poling geometry," *J. Appl. Phys.*, **73**, 8471-8479, 1993.
(52) H.L Hampsch, J. Yang, G.K. Wong, J.M. Torkelson, "Dopant orientation dynamics in doped second-order nonlinear optical amorphous polymers. 1. effects of temperature above and below $T_g$ in carona-polled films," *Macromolecules*, **23**, 3640-3647, 1990.